J. Membrane Biol. 154, 109–118 (1996)

The Journal of
Membrane
Biology

Modeling Plasmalemma Ion Transport of the Aquatic Plant *Egeria densa*

P. Buschmann, H. Sack, A.E. Köhler, I. Dahse
Friedrich-Schiller-Universität Jena, Biologisch-Pharmazeutische Fakultät, Institut für Biochemie und Biophysik, Philosophenweg 12, D-07743 Jena

Received: 18 March 1996/Revised: 17 July 1996

Abstract. Fresh-water plants generate extraordinarily high electric potential differences at the plasma membrane. For a deeper understanding of the underlying transport processes a mathematical model of the electrogenic plasmalemma ion transport was developed based on experimental data mainly obtained from *Egeria densa*. The model uses a general nonlinear network approach and assumes coupling of the transporters *via* membrane potential. A proton pump, an outward-rectifying K^+ channel, an inward-rectifying K^+ channel, a Cl^- channel and a $(2H\text{-}Cl)^+$ symporter are considered to be elements of the system. The model takes into consideration the effects of light, external pH and ionic content of the bath medium on ion transport. As a result it does not only satisfactorily describe the membrane potential as a function of these external physiological factors but also succeeds in simulating the effects of specific inhibitors as well as *I-V*-curves obtained with the patch-clamp technique in the whole cell mode. The quality of the model was checked by stability and sensitivity analyses.

Key words: *Egeria densa* — Ion transport — Membrane potential — Plasmalemma — Simulation model — Light

Introduction

Egeria densa Planchon, formerly *Elodea densa* Caspary, is a higher aquatic plant belonging to the *Hydrocharitaceae*. It has been a preferred material for different studies in plant physiology such as cyclosis, oxygen evolution or ion transport for a long time. Electrophysiologists have taken advantage of the thin leaves consisting of two layers of cells only and allowing studies at the whole undamaged organ in a natural environment. They also esteem *Egeria* as one of the model organisms of the plant kingdom because of remarkable phenomena related to ion transport such as leaf polarity [24, 57, 58, 76] and values of the electric potential difference at the plasmalemma of up to ca. −300 mV in the light. On the other hand, they had to accept the disadvantage that due to very close cell-cell contacts *via* plasmodesmata [28, 66] informative *I-V*-curves could not be obtained from single cells. In the last decade detailed experimental data related to plasmalemma ion transport have been accumulated (e.g. [17, 20, 23, 41, 46, 49, 54, 69]). In this context, the desire to integrate these data into an overall picture of cellular transport to compensate for the lacking *I-V* curves emerged. For developing a transport model for *Egeria* leaf cells we used the following prominent features observed in this plant:

(i) The membrane potential is very sensitive to changes in light intensity at acid or neutral medium pH. In contrast to the *Characeae* [32] in *Egeria* leaf cells, dark/light transitions always cause a hyperpolarization of the membrane potential. The kinetics of these transitions can be divided into three phases: A short depolarization of a few millivolts is followed by a steep hyperpolarization. Before reaching the light-adapted steady state usually a slight depolarization occurs (Fig. 1). Under linearizing conditions, the kinetics can be described by a sum of exponentials [37]. A time constant τ_i for each of the three phases could be determined ($\tau_1 = 29.5$ sec, $\tau_2 = 264$ sec, $\tau_3 = 307$ sec) [14] and was then used in the model (Eqs. 11). At high medium pH (>8) the light sensitivity of the membrane potential disappeared [19].

(ii) Another remarkable feature of *Egeria* leaf cells is the disappearance of the dependence of the membrane potential on external KCl concentration and light condi-

Dedicated to: Prof. Dr. Eberhard Müller on the occasion of his 65th birthday.

Correspondence to: P. Buschmann

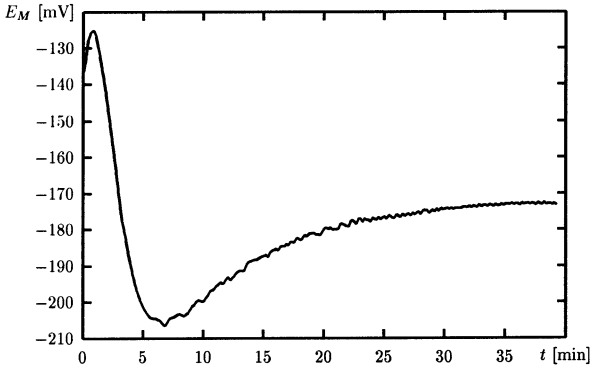

Fig. 1. Effect of a dark/light transition on the measured membrane potential of a dark-adapted *Egeria* leaf cell. Light was switched on at $t = 0$.

tions at strong alkaline external pH (Fig. 2). Between pH values of 5.5 to 7.5 there is a clear KCl dependence of the membrane potential according to the Goldman-Hodgkin-Katz equation [39]. For pH >8 this dependence is vanishing together with the light reaction (hyperpolarization) of the membrane potential. The importance of this phenomenon is enhanced by experimental findings that under strong illumination *Egeria* leaf cells acidify the medium on the abaxial side of the leaf and alkalize the adaxial side of the leaf.

These and other data give evidence for a complex regulation of plasmalemma ion transport and membrane potential in response to environmental conditions. After giving a condensed description of our model, for details see [14], we here present results of simulations and implications for ion transport in *Egeria* leaf cells.

Materials and Methods

Culture Conditions and Experimental Setup

Egeria plants were grown in an aquarium with a soil-covered ground filled with tap-water under artificial illumination (7 W/m^2, neon tube) in a light/dark regime of 12 hr. Temperature was held constant at 18°C. Prior to microelectrode impalements fully differentiated leaves were isolated and mounted in a plexiglass chamber adapted to a Zeiss Jenalumar microscope. Membrane potential measurements were performed as described elsewhere [18] with the following modifications: The signal was amplified using a WyeScience μP amplification system. The data were recorded on IBM-PC microcomputer, equipped with an A/D interface (AT M/O-16-9L, National Instruments).

The kinetic analysis of the light effect was performed by using the so-called 1X-solution (1 mol/m^3 KCl, 1 mol/m^3 $Ca[NO_3]_2$, 0.25 mol/m^3 $MgSO_4$, 1 mol/m^3 Na_2HPO_4/NaH_2PO_4 buffer, pH 5.9). For the experiments with variation of external pH (5.5–9.5) and KCl concentration (10/1/0.1 mol/m^3 KCl) under dark and light conditions the following bath medium was used: 1 mol/m^3 NaCl, 1 mol/m^3 $CaCl_2$, 0.25 mol/m^3 $MgCl_2$, 10.0 mol/m^3 1,3-bis[tris(hydroxymethyl)methylamino]propane buffer for pH adjustment.

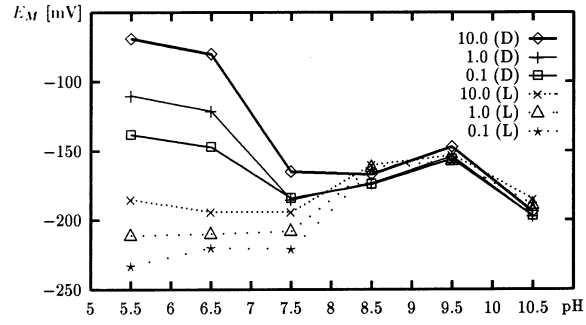

Fig. 2. Measured dependence of the membrane potential on external pH (5.5–9.5) and KCl concentration (10/1/0.1 mol/m^3 KCl) under dark (D) and light (L) conditions.

Kinetic Analysis of the Light Effect on Membrane Potential

Under linearizing conditions the response of the membrane potential $h(t)$ to a stepwise change in light intensity can be described by a sum of exponentials [37]

$$h(t) = A_o + \sum_{i=1}^{n} A_i \cdot (1 - exp\ (-t/\tau_i)). \tag{1}$$

Curve-fitting of measured data $y(t)$ to the function $h(t)$, which means minimizing the sums of squares

$$M(A_i, \tau_i) = \sum_{j=1}^{m} (y(t) - h(t))^2, \tag{2}$$

is a notoriously ill-conditioned problem [1]. Furthermore, we have to take into consideration that most algorithms find only local minima. To overcome this problem we used a hybrid algorithm [27], which combines an evolutionary strategy [64] with a simplex method [53]. The fitting procedure was started with the evolutionary strategy. Once the range of the global minimum was found, the optimal parameter values were extracted by the simplex method. Additionally, advantage was taken of the linear occurrence of the amplitude factors A_i in Eq. 1. So it was possible to adjust the parameters A_i by solving the linear system

$$\frac{\partial\, M(A_i, \tau_i)}{\partial\, A_i} = 0 \tag{3}$$

under temporary fixing of the time constants τ_i. Using sets of test data it has been verified that the hybrid algorithm is able to calculate the optimal parameters with satisfactory precision [14].

The time constants and amplitude factors achieved by this procedure are shown in Appendix 2; Table A4. The time constants were used in the modeling of the light-dependent transient kinetics of the membrane potential (*see* Eq. 11). The metabolite amplitude factors K_i (Appendix 2; Table *A*2) were assumed to be proportional to the voltage amplitude factors. A_i (Appendix 2, Table *A*4).

The Model

Because of the lack of convincing *I-V* curves and the including of transient processes it was not possible to use some kind of state models [10, 26, 33, 62].

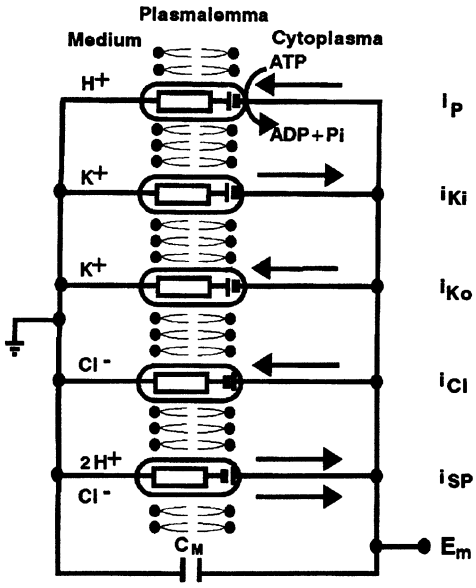

Fig. 3. A simplified equivalent circuit model of the plasma membrane.

The description of our model is divided into three parts:

1. Scope of the model
2. Basic model
3. Extensions and modifications of the basic model

Scope of the Model

In view of the numerous plasmalemma ion transporters it was necessary to confine the number of elements in the model to a few essential processes. According to our experimental results and to data from the literature, we assumed that a minimal configuration must consist of a proton pump, a K^+-inward rectifier, a K^+-outward rectifier, a $(2H\text{-}Cl)^+$ symporter, and a Cl^- channel (Fig. 3). We will call all these elements transporters in the following. Current knowledge suggests them to be the basic equipment of fresh-water plant cells.

Whereas there is general agreement on the existence of the plasmalemma proton pump and the channels there is no direct evidence for a (2H-Cl)+ symporter in *Egeria* leaf cells until now. However, the relatively high cytoplasmic Cl^- concentration ([17]: 46 mM) requires some anion uptake system. Due to the outwardly directed thermodynamic driving force for chloride ions such an uptake can not be managed in a passive way. In addition, an anion uptake under illumination even at external concentrations of 0.1 mM Cl^- was reported [40, 75], which can be accomplished only by an electrogenic cotransport system. Therefore, we included in our model a $(2H\text{-}Cl)^+$ symporter as described for *Characeae* [3, 59, 60]. The lack of data may be explained by the fact that the small changes due to this symport are difficult to detect against the background of the proton pump and the assembly of channels [3, 17]. A detailed discussion of gradient-coupled chloride transport in plant cells can be found in [61].

Basic Model

For an appropriate description of ion transport we used an approach which was developed by Gradmann and successfully applied to the description of phenomena like action potentials and nonlinear oscillations [29, 30, 51, 70]. Accordingly, the model transporters are characterized by open probabilities (P_i) which are dependent on the membrane potential. The dynamic change of an open probability reflects the transition between the active and inactive state, which takes place over a symmetric Eyring barrier with the transition probabilities k^i (inactivation) and k^a (activation):

$$dP_i/dt = -k_i^i \cdot P_i + k_i^a \cdot (1 - P_i) \tag{4}$$

with

$$k_i^a = \hat{k}_i^a \cdot \exp(\delta_i^a \cdot FE_M/(RT)) \tag{5}$$

and

$$k_i^i = \hat{k}_i^i \cdot \exp(\delta k_i^i \cdot FE_M/(RT)). \tag{6}$$

The parameter δ contains the portion of the membrane potential which is effective, the charge number of the gating particle and a geometric factor for the shape of the energy barrier [30]. The range of δ was restricted to ± 0.5 due to the assumptions of unity 'gating-charges' and symmetry of the energy barriers. The sign of δ determines the direction of activation of a transporter. If a positive-going membrane potential activates a transporter, then in the model $\delta^a = 0.5$ has to be chosen. Correspondingly, if a negative-going membrane potential activates a transporter, $\delta^a = -0.5$ is required. $\hat{k}_i$ are the transition probabilities at zero voltage. F, R and T have their usual thermodynamic meanings. By applying Eq. 4 to each of the five transporters we obtain a system of differential equations which can be solved with appropriate numerical methods. The conductance of each transporter is the product of its maximum conductance and the actual open probability:

$$g_i = g_i^{\max} \cdot P_i. \tag{7}$$

If the equilibrium voltages E_i and the membrane capacitance C_M (1 $\mu F/cm^2$) are known, the current densities and the membrane potential can be obtained:

$$i_i = g_i \cdot (E_M - E_i) \tag{8}$$

$$dE_M/dt = 1/C_M \cdot \Sigma i_i. \tag{9}$$

This general approach was modified to include the effect of environmental factors in the simulation of the membrane transport.

Extensions and Modifications of the Basic Model

Modeling the Plasmalemma Proton Pump. In plants the activity of the plasmalemma H^+-ATPase is directly or indirectly influenced by a huge number of factors [47, 48, 65]. In the case of *Egeria* leaf cells this proton pump is mainly effected by light [17, 45, 69]. This experimental finding was taken into account in the model by the assumption of a proportional relation between steady-state activity of the proton pump P_P^s and an activation parameter $\mathcal{L}_{\mathcal{A}}$ reflecting light intensity

$$P_P^s = K \cdot \mathcal{L}_{\mathcal{A}}. \tag{10}$$

For the simulation of the transient kinetics of membrane potential (Fig. 1) caused by a stepwise change of light intensity it was assumed that light acts on the proton pump *via* three generalized pathways (Fig. 4). By measurements with pH-sensitive microelectrodes it could be shown that for *Egeria* leaf cells [54] like for other photosynthetic plant cells the first depolarizing phase of the kinetics is connected with a short increase in cytosolic pH. These findings were analyzed in detail by Hansen and coworkers [36, 37, 72, 74]. They found that this transient alkalinization of the cytosol (caused by photosynthetic uptake of

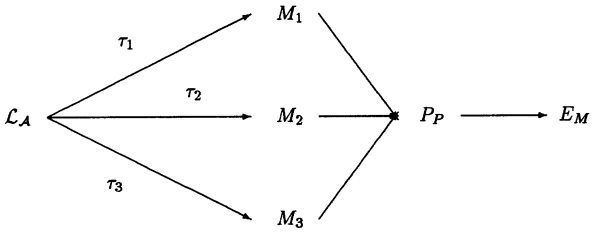

Fig. 4. Diagram for the light effect on the proton pump *via* three generalized pathways. An increase in light intensity (simulated by an increased activation parameter $\mathcal{L}_{sA}$) results in a proportional rise in the concentrations of the generalized metabolites M_i with a time delay which is characterized by the time constants τ_i. As a net effect of this increase, a hyperpolarization of the membrane potential E_M caused by an activation of the plasmalemma proton pump occurs (P_P: open probability of the pump).

protons into the thylakoid lumen) is slowing down the ATP-driven plasmalemma proton pump and as a result the membrane potential is depolarized. The second phase of the kinetics which is responsible for the hyperpolarizing net effect of the light reaction is also mediated by the plasmalemma H^+ pump. This could be verified by application of specific inhibitors and measurements of H^+ extrusion [17, 46] as well as by kinetic analysis [37]. The third phase of the kinetics is not well examined yet. At present a further effect from photosynthesis to the proton pump seems to be most likely. An alternative would be an influencing of a potassium channel [73]. However, the time constant τ_3 of the third phase of the kinetics is considerably greater than comparable data [37]. Besides this, preliminary experiments with potassium channel blockers indicate no significant effect on the kinetics.

In the model the three pathways introduced (Fig. 4) were described by a parallel arrangement of proportional elements with time delay

$$dM_i/dt = -1/\tau_i \cdot M_i(t) + K_i/\tau_i \cdot \mathcal{L}_{sA}, \; i = \overline{1, 3} \tag{11}$$

M_1 is essentially an abstraction of pH_{cyt}. Increasing cytosolic pH can cause an inactivating effect on the proton pump in several ways. Firstly, the equilibrium potential of the protons (E_H) is changed and hence also the thermodynamic driving force of the proton pump ($E_M - E_P$) (Eq. 30). Secondly, it has to be considered that maximal activity of the proton pump can be found at a cytosolic pH of 6.5 [31]. This means that an increased cytosolic pH gives rise to a reduced activity of the pump. Thirdly, also the pH_{cyt} dependence of the free energy of ATP-hydrolysis ΔG_{ATP} has to be taken into account. The nature of M_2 is under discussion. For *Egeria* the NADPH/$NADP^+$-ratio seems to play an essential role [23, 48]. The identity of M_3 is still unknown.

In the case of the proton pump, Eq. 11 replaces the rate Eq. 4 of the basic model. This means that a stepwise change in light intensity causes a proportional increase of the generalized metabolite concentrations M_i. In addition, a proportional relation between the activity of the proton pump and the generalized metabolite concentrations was assumed

$$P_P(t) = K \cdot \Sigma M_i(t), \; i = \overline{1, 3} \tag{12}$$

Influence of External Ion Concentration. For the simulation of varying external ion concentrations not only resulting changes of the reversal potentials of the ion transporters but also changes of the corresponding conductances have to be considered. These conductances may be influenced by external KCl concentration as well as by external pH. Therefore the maximum conductances g_i^{max} were calculated as products of the basic maximum conductances g_i^0 and the corresponding pH-dependent conductance factors γ_i

$$g_i^{max} = g_i^0 \cdot \gamma_i. \tag{13}$$

The basic maximum conductances g_i^0 were assumed to be 1 S/m^2 for the H^+ transporters. Estimations for the basic maximum conductances of the K^+ and Cl^- transporters, which are influenced by the potassium and chloride concentrations of the external solution, respectively, were calculated according to the constant field theory [63]

$$g_i = -\frac{P_i z_i^2 F^2 \xi_i}{RT} \cdot \frac{(c_i^{ext} - c_i^{cyt} e^{\xi_i})}{(1 - e^{\xi_i}) \cdot (\xi_i - ln(c_i^{ext}/c_i^{cyt}))} \text{ with } \xi_i = z_i F E_M/RT. \tag{14}$$

The dependence of the membrane transport on extracellular pH was taken into consideration by conductance factors γ_i. Following the model of Miedema and Prins [50] it was assumed that the H^+ transporter is working in pump mode at low pH and in channel mode at high pH. The pH-dependent ration of proton channel and pump conductances was calculated as

$$\alpha_1 = \beta \cdot 10^{n \cdot (pH - pK_1)} \tag{15}$$

with $\beta = 10$ (ratio of channel and pump conductances on a microscopic scale), $n = 2$ (number of protonation steps) [50]. Then it was used for determination of the maximum conductances of the H^+ transporter in pump mode g_P^{max} and in channel mode g_H^{max} (*see also* Fig. 5)

$$\gamma_P = \frac{1}{\alpha_1 + 1}, \qquad \gamma_H = 1 - \gamma_P. \tag{16}$$

In addition, the variable H^+/ATP stoichiometry s of the proton pump was adopted from Miedema and Prins [50]. The stoichiometry shifts from a value from $s = 1$ at pH = 5.5 to $s = 2$ at pH = 10.5.

Because of the experimental observation that for $pH > 8$ the membrane potential is insensitive to KCl concentration (Fig. 2) we assumed an inactivation of the K^+ and Cl^- transporters under these conditions

$$\alpha_2 = \beta \cdot 10^{n \cdot (pH - pK_2)} \tag{17}$$

$$\gamma_i = \frac{1}{\alpha_2 + 1}, \qquad i \in \{K_i, K_o, Cl, SP\}. \tag{18}$$

The subscript i indicates the corresponding plasmalemma ion transporter (see Fig. 3).

The main model equations and model parameters are summarized in Appendix 1 and 2, respectively. Further details of the *Egeria* model can be found elsewhere [14].

Results

The simulation of different transport situations confirms that the model is able to reproduce the experimental data fairly well. In Figs. 6–8 the simulated effects of light, medium pH and ionic content of bath medium on membrane transport are shown.

Figure 6 compares measured and calculated steady-state membrane potential values in dependence on light intensity $\mathcal{L}$ and the activation parameter $\mathcal{L}_{sA}$, respectively. For a better understanding of the figure it has to be mentioned that in darkness two different steady states could be observed experimentally. In the case of a pre-

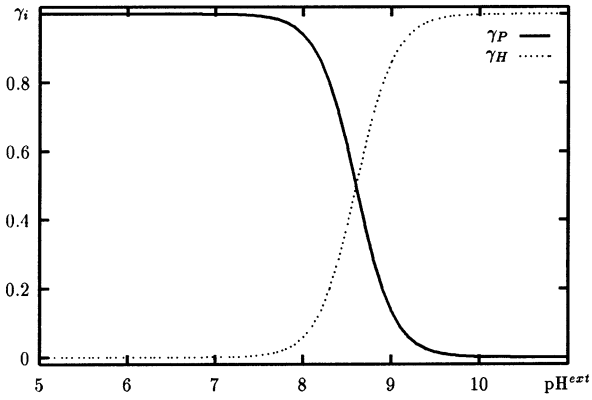

Fig. 5. Regulation of the operation mode of the plasmalemma H^+ transporter by the external pH according to Eqs. 15 and 16 with $pK = 9.1$. The active (pump) mode dominates for pH < 8, while the passive (channel) mode becomes significant for pH > 9.

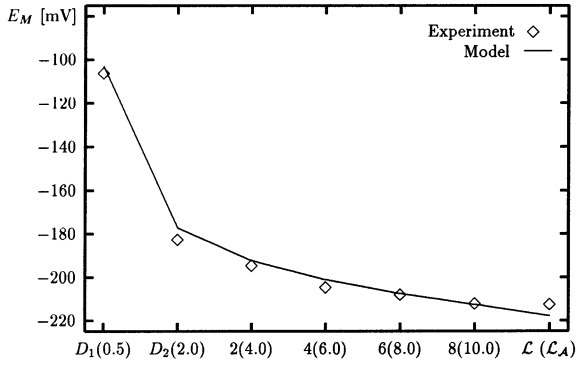

Fig. 6. Comparison of measured and calculated steady-state membrane potential values in dependence on light intensity $\mathcal{L}$ [W/m^2] (experimental) and the activation parameter $\mathcal{L}_{sA}$ (model) respectively.

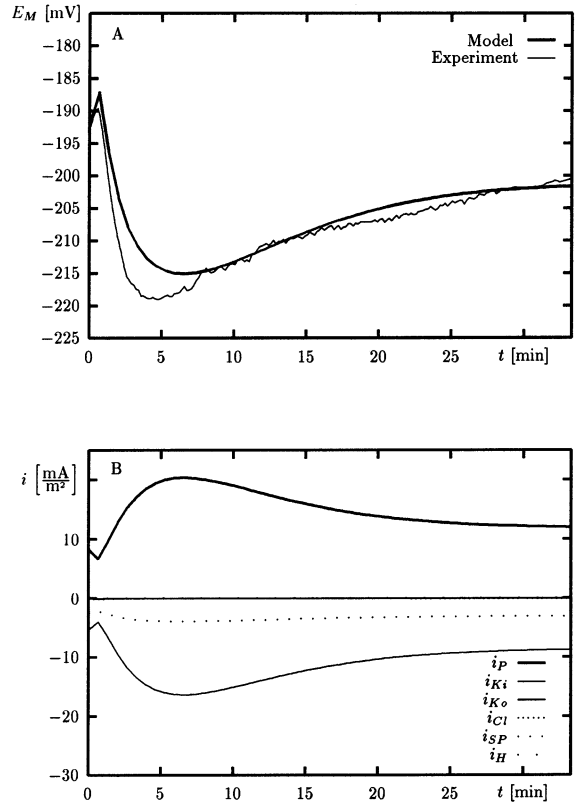

Fig. 7. Experimental and simulated effect of a dark/light transition on membrane potential under linearizing conditions (*A*) and on the corresponding simulated current densities (*B*). Light intensity was changed at $t = 0$ from $\mathcal{L} = 2$ W/m^2 to $\mathcal{L} = 4$ W/m^2. In correspondence with experimental data the simulation yields an enhanced proton pumping and thereby a higher uptake of potassium and chloride ions with increasing light intensity. i_{Ko}, i_{Cl} and i_H are zero.

treatment with high light intensity (>10 W/m^2), steady-state values of the membrane potential more positive than the equilibrium potential of the potassium ions, E_K, were measured in the dark (denoted by D_1). If, however, a lower light intensity (3 W/m^2) was applied before darkness, a steady state considerably more negative than E_K was obtained (denoted by D_2). In the D_1 state the membrane potential usually repolarizes spontaneously to the D_2 state after 30 to 60 min under continuing darkness. This transition is ascribed to an increase of the proton pump rate due to respiration. For the modeling we had furthermore to take into consideration that the proton pump in darkness is not completely inactivated [16, 45, 50]. So the parameter $\mathcal{L}_{sA}$ was set to 0.5 for the D_1 state and to 2.0 for the D_2 state. For the light states the $\mathcal{L}_{sA}$ values were increased parallel to light intensity.

The model can also be used to simulate the transient membrane potential kinetics caused by a stepwise change in light intensity (Fig. 7). In Fig 7*B* the simulated current densities are shown. In correspondence with experimental data [46, 75] the simulation yields an enhanced proton pumping and thereby a higher uptake of potassium and chloride ions with increasing light intensity.

The simulated pH and KCl dependences of the membrane potential under dark and light conditions are presented in Fig. 8. In accordance with the experimental data (Fig. 2), for pH > 8 a convergency of the steady-state potential values can be seen. In the case of a further increase of the pH above 9.5 the calculated membrane potential values follow the values of E_H as it was observed on *Characeae* [5].

Recently, it was possible to measure *I-V*-curves from *Egeria* protoplasts by means of the patch-clamp technique in the whole cell mode (Fig. 9*A*) [52]. These data gave rise to an examination of the model under voltage-clamp conditions. The simulation (Fig. 9*B*) showed in accordance with the experimental values a significant decrease in the membrane current.

Every biological system must be able to cope with disturbances for surviving. This is valid also for ion

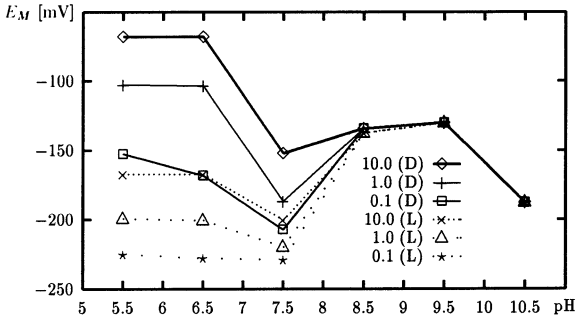

Fig. 8. Simulated medium pH- (5.5–9.5) and KCl-dependence (10/1/0.1 mol/m^3 KCl) of the membrane potential under dark (D) and light (L) conditions. In comparison with the experimental data (Fig. 2) a satisfactory correspondence is achieved. The following parameter values were used: D: $\mathscr{L}_{\mathscr{A}} = 0.5$, $pK_1 = 9.1$, $pK_2 = 7.6$, L: $\mathscr{L}_{\mathscr{A}} = 6.0$, $pK_1 = 8.6$, $pK_2 = 7.6$.

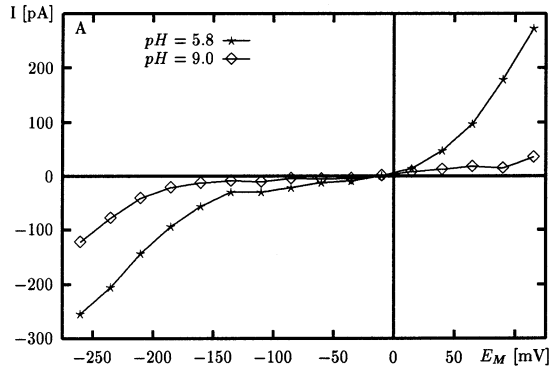

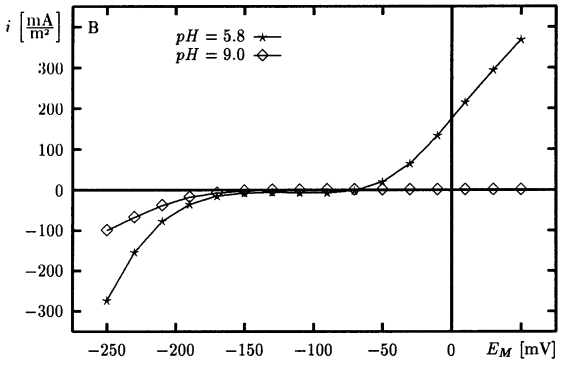

Fig. 9. Experimentally determined *I-V*-curves from an *Egeria* protoplast measured by means of the patch-clamp technique in whole cell modus [52] (*A*) in comparison with simulated *I-V*-curves according to the model (*B*).

transport processes. So we had to verify whether the proposed model satisfies stability requirements. From a mathematical point of view, stability analysis can be done by linearization of the system at the steady state and calculation of the eigenvalues of the linearized system

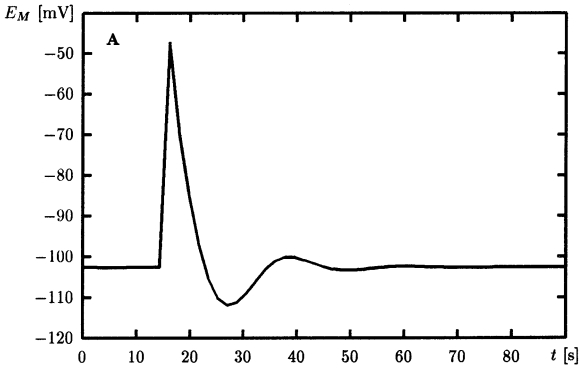

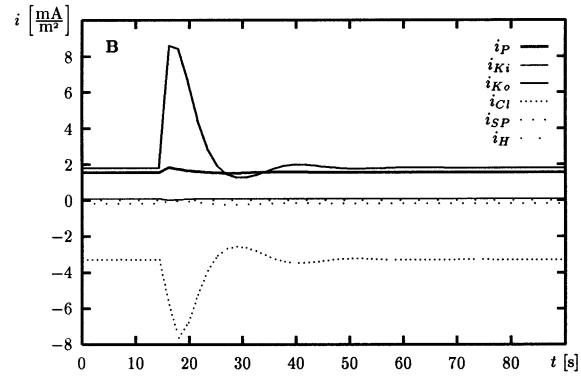

Fig. 10. Simulated response of the membrane potential (*A*) and the current densities (*B*) on a disturbance (depolarization) caused by an additional leak current (*not shown*) in darkness.

[21]. In this way the stability of the steady states in Figs. 6–10 was checked. The stable behavior of the model can be illustrated by various examples. In Fig. 10 a simulated disturbance (depolarization) of the membrane potential in darkness is shown. It could be caused by a short injury of the membrane or by an electrogenic uptake of organic molecules *via* a proton-driven symporter [55]. After the disturbance the system relaxes into the initial state. In a similar manner, a partial blocking of the K^+-channels can be simulated. In accordance with experimental data obtained from *Egeria* leaf cells [13] blocking of the K^+-inward rectifier and of the K^+-outward rectifier results in a hyperpolarization and a depolarization, respectively.

Besides stability, which characterizes the ability of a system to compensate small disturbances of the variables, also the sensitivity to small changes of the parameter values is an important feature of a model [15]. For our model it was found that the steady states in darkness were more parameter-sensitive than the steady states in the light. The reason for this are the feedback features of the ion transporters. Except for the proton pump they are voltage-dependent (Eqs. 5 and 6) and influence for their part the membrane voltage (Eq. 9). We can distinguish

two cases: Either activation of an ion transporter shifts the membrane potential in such a way that the transporter is inactivated (negative feedback) or the change of the membrane potential results in a further activation of the transporter (positive feedback). Negative feedback mechanisms have a stabilizing effect and positive feedback mechanisms a destabilizing effect on the overall system. In our model, all the transporters except the anion channel realize negative feedback mechanisms leading to a stable behavior of the overall system. However, in darkness especially at E_M near E_K, the anion currents can reach a relatively high influence. In this situation the sensitivity of the model towards parameter changes is enhanced because of the destabilizing properties of the anion channel. As a result of the sensitivity analysis it may be speculated that the anion channel has a third state as it was found in other plants [29, 51, 70]. This additional state would inactivate the channel in the case of positive-going membrane potential, turning this transporter into a stabilizing element.

Discussion

Simulations using the model presented here confirm and explain electrophysiological results obtained from *Egeria* leaf cells: The high electrogenicity of the plasmalemma H^+ ATPase is crucial for the electrophysiological phenomena in *Egeria*. In the light, this proton pump hyperpolarizes the cell membrane (Fig. 7) and acidifies the medium at the lower leaf side, thereby providing the driving force for electrogenic membrane transport. At alkaline pH, the pump is deactivated despite illumination. Due to numerous plasmodesmata, the membrane potential of all leaf cells is clamped at the same value. The main antagonist of the plasmalemma proton pump is the inward-rectifying K^+ channel. It opens at hyperpolarizing membrane potentials allowing potassium uptake. In principle, H^+/X symporters are also antagonists of the proton pump though of less influence on the membrane potential (Fig. 7*B*). In darkness, the plasmalemma ATPase pumps protons out of the cell at a low rate. This leads to a depolarized state in comparison to the cell potential in the light. In the case of a depolarization to values more positive than in the D_1 state (caused, e.g., by temporary membrane damage or energy depletion) the K^+-outward rectifier is activated (Fig. 10). This mechanism can be regarded as a kind of buffering of the plasmalemma potential difference, which is necessary for many cell processes. Critical potassium loss in the D_1 state will be limited for two reasons: (i) The conductance of the other ion transporters is very low in this state [49]. (ii) The D_1 state will spontaneously turn into the D_2 state under continuing darkness. In this way *Egeria* seems to accomplish balanced osmotic relations.

The effect of light on the membrane potential in plants was examined by Hansen and coworkers in detail [36, 37, 72, 74]. They found at least four different pathways for the action of photosynthetic processes on plasmalemma ion transport. Both of the corresponding time constants concerning the action on the plasmalemma proton pump were also found in *Egeria* leaf cells (Appendix 2; Table *A*4). The difference in the other time constants may be due to different experimental conditions or the variability of the ion transporters (e.g., different kind of K^+ channels).

In addition to the influence of light, plasmalemma ion transport is regulated by medium pH [11, 38, 71]. In our model, both K^+ channels are activated by hyperpolarizing (inward-rectifying K^+ channel) or depolarizing voltage (outward-rectifying K^+ channel) at acid or neutral extracellular pH, respectively. As a consequence there is a significant influence of the K^+ concentration of the bath medium on the membrane potential in the light as well as in darkness. With increasing external pH first the K^+ and Cl^- transporting devices (Eqs. 17 and 18) inactivate and then the plasmalemma proton pump turns into the channel mode (Eqs. 15 and 16). So the proton pump most strongly predominates at pH 7.5 resulting in a hyperpolarized membrane potential. Between pH 8.5 and 9.5 the membrane potential remains nearly unchanged due to the opposite-directed processes of inactivation of the proton pump and activation of the passive H^+ conductance (E_H becomes more negative with increasing pH). For strong alkaline pH, the membrane potential is approaching the reversal potential of the passive H^+ transporter. These dependencies can be seen in simulations using our transport model (Fig. 8); they reflect electrophysiological results where the experimentor determines the medium pH.

The question arises as to how and for what purpose *Egeria* leaves develop leaf polarity including an acid pH at the lower leaf side and an alkaline pH at the upper side. The purpose seems clear since the uptake of inorganic carbon has been investigated in *Characeae* and *Hydrocharitaceae* (*reviews*: [42, 44, 57]). In both cases a bicarbonate utilization was found. At high light intensities and low dissolved carbon concentration these fresh-water plants generate a low pH at certain regions (alkaline bands in the *Characeae* [8], the adaxial leaf side in *Hydrocharitaceae*) [24] for CO_2 uptake. The acidification shifts the equilibrium of the carbon dioxide system towards CO_2, which then enters the cell by passive diffusion [56, 67]. Another proposed mechanism for bicarbonate utilization is an H^+/HCO_3^- symporter located in the plasmalemma [25, 43].

The pH polarity of *Egeria* leaf cells is mainly established by the H^+ transporters, which are working in the pump mode or in the channel mode in dependence on the external pH [50]. The pivotal question is how the mode of the H^+ transporter is switched, i.e., how a change of

the medium pH is triggered. Elzenga and Prins [22] proposed a model for the generation of pH polarity for *Hydrocharitaceae* assuming a positive feedback system: with rising pH at the leaf surface the proton transporter switches from the pump to the channel mode resulting in a further rise of the pH value. To make this feedback system work, an initial trigger impulse must be provided. The nature of this impulse is still in discussion, but there are at least three possibilities: (i) A small imbalance in the proton fluxes was proposed due to the asymmetric distribution of the plasmalemma ATPase [22]. (ii) A transient activation of the K^+-inward rectifier caused by the initial depolarization after switching on the light would be possible. (iii) A transient uptake of anions by means of a proton symporter, which is energized by the light-induced hyperpolarization could be imagined. The first hypothesis is difficult to set in accordance with acid-base theory [68] which states that the pH cannot be changed by a net proton flux but only by an accompanying net flux of strong ions (e.g., K^+ or Cl^-). All proposals require a heterogeneous distribution of the corresponding transporters, preferentially located in the plasmalemma of the lower (ATPase) or upper (inward-rectifying K^+ channel and proton-driven anion symporter) leaf side. Nevertheless, the pH polarity enables the cell to ensure an optimum supply with inorganic carbon and the homeostasis of cytoplasmic pH.

To sum up, the model is able to describe the plasmalemma ion transport of *Egeria* leaf cells as determined by a framework of H^+, K^+, and Cl^- transporters. The proton pump, which is controlled by photosynthesis, establishes an H^+ electrochemical gradient. This gradient provides the driving force for gradient-coupled transport systems. The ion channels considered catalyze dissipative transport for ion uptake or maintenance of the membrane potential. The membrane potential is dominated by the proton pump (pump state) in the light at acid or neutral medium pH, under strong depolarized conditions by the K^+-outward rectifier (K^+ state) and at high medium pH by the passive H^+ conductance (H^+ state). These states, which were first described for *Characeae* [4, 6, 9], can be simulated by means of our model. They are suggested as general patterns of ion transport across the plasmalemma of fresh-water plants for adaptation to changing environmental conditions.

We are grateful to Prof. D. Gradmann (Göttingen) and Prof. U.-P. Hansen (Kiel) for critical comments and helpful discussions. Furthermore, we would like to thank Ms. Heidi Traber for technical assistance.

References

1. Acton, F.S. 1970. Numerical Methods that (Usually) Work. p. 253. Harper & Row, New York
2. Beffagna, N., Romani, G. 1991. Modulation of the plasmalemma proton pump activity by intracellular pH in *Elodea densa* leaves: Correlation between acid load and H^+ pumping activity. *Plant Physiol. Biochem.* **29:**471–480
3. Beilby, M.J., Walker, N.A. 1981. Chloride transport in *Chara. J. Exp. Bot.* **32:**43–54
4. Beilby, M.J. 1990. Current-voltage curves for plant membrane studies. A critical analysis of the method. *J. Exp. Bot.* **41:**165–182
5. Beilby, M.J., Bisson, M.A. 1992. *Chara* plasmalemma at high pH. *J. Membrane Biol.* **125:**25–39
6. Beilby, M.J., Mimura, T., Shimmen, T. 1993. The proton pump, high pH channels, and excitation: voltage clamp studies of intact and perfused cells of *Nitellopsis obtusa. Protoplasma* **175:**144–152
7. Bentrup, F.W. 1985. Botanische Elektrophysiologie. *Naturwissenschaften* **72:**169–179
8. Bisson, M.A., Walker, N.A. 1980. The *Chara* plasmalemma at high pH. *J. Membrane Biol.* **56:**1–7
9. Bisson, M.A., Walker, N.A. 1982. Transitions between modes of behavior (states) of the charophyte plasmalemma. *In:* Plasmalemma and tonoplast: Their Functions in the Plant Cell. D. Marmé, E. Marré, and R. Hertel, editors. pp. 35–40. Elsevier, Amsterdam
10. Blatt, M.R., Beilby, M.J., Tester, M. 1990. Voltage dependence of the *Chara* proton pump revealed by current-voltage measurements during rapid metabolic blockade with cyanide. *J. Membrane Biol.* **124:**205–223
11. Blatt, M.R. 1992. K^+ channels of stomatal guard cells. *J. Gen. Physiol.* **99:**615–644
12. Briskin, D.P., Hanson, J.B. 1992. How does the plant plasma membrane H^+-ATPase pump protons? *J. Exp. Bot.* **43:**269–289
13. Buschmann, P., Kuschel, L., Dahse, I., Köhler, A.E. 1993. Ion transport across the plasma-lemma of *Egeria* leaf cells. In: Membrane Transport in Plants and Fungi: Molecular Mechanisms and Control. Symposium of SEB and FESPP, 12.9–15.9.1993, p. 25 Wye, UK
14. Buschmann, P. 1996. Ein Modell für den Ionentransport über die Plasmamembran der Wasserpflanze *Egeria densa*. Friedrich-Schiller-Universität Jena, Dissertation
15. Cruz, J.B. 1973. System Sensitivity Analysis. Dowden, Stroudsburg
16. Cruz-Mireles, R.M., Ortega-Blake, I. 1991. Effect of Na_3VO_4 on the P-State of *Nitella translucens. Plant Physiol.* **96:**91–97
17. Dahse, I., Linsel, G., Müller, E., Dawczynski, H., Opfermann, J. 1987. The membrane potential as indicator for transport and energetic processes of leaf cells I. *Biochem. Physiol. Pflanzen.* **182:**117–128
18. Dahse, I., Sack, H., Bernstein, M., Petzold, U., Müller, E., Vorbrodt, H.M., Adam, G. 1990. Effects of (22S, 23S)-homobrassinolide and related compounds on membrane potential and transport of *Egeria* leaf cells. *Plant Physiol.* **93:**1268–1271
19. Dahse, I., Traber, H., Kuschel, L., Sack, H., Müller, E. 1994. Potassium independence of the electric cell potential at alkaline pH in *Egeria densa. In:* Botanikertagung, 11.9–19.9. 1994 p. 322. Bayreuth
20. De Boer, A.H., Miedema, H., Giesberg, H., Prins, H.B.A. 1992. Patch clamp studies on *Elodea* leaf protoplasts. *In:* 9th International Workshop on Plant Membrane Biology, p. 141. Monterey, CA
21. Edelstein-Keshet, L. 1988. Mathematical Models in Biology. pp. 113–163. Random House, New York
22. Elzenga, J.T.M. 1989. The mechanism for bicarbonate utilization in water plants. Groningen, Thesis. pp. 117–126
23. Elzenga, J.T.M., Staal, M., Prins, H.B.A. 1989. ATPase activity of isolated plasma membrane vesicles of leaves of *Elodea* as affected by thiol reagents and NADH/NAD^+ ratio. *Physiol. Plant.* **76:**379–385

24. Elzenga, J.T.M., Prins, H.B.A. 1989. Light-induced polar pH changes in leaves of *Elodea canadensis. Plant Physiol.* **91:**62–67
25. Fisahn, J., Lucas, W.J. 1992. Direct measurement of the reversal potential and current-voltage characteristics in the acid and alkaline regions of *Chara corallina. Planta* **186:**241–248
26. Fisahn, J., Hansen, U.-P., Lucas, W.J. 1992. Reaction kinetic model of a proposed plasma membrane two-cycle H^+-transport system of *Chara corallina. Proc. Natl. Acad. Sci. USA* **89:**3261–3265
27. Goldberg, D.E. 1989. Genetic algorithms in search, optimization and machine learning. p. 74. Addison-Wesley, Reading, MA
28. Goodwin, P.B. 1983. Molecular size limit for movement in the symplast of the *Elodea* leaf. *Planta* **157:**124–130
29. Gradmann, D., Blatt, M.R., Thiel, G. 1993. Electrocoupling of ion transporters in plants. *J. Membrane Biol.* **136:**327–332
30. Gradmann, D., Buschmann, P. 1996. Electrocoupling causes oscillations of ion transporters in plants. H. Greppin, M. Banzon, R. DegliAgosti, editors. University of Geneva (*in press*)
31. Hager, A., Biber, W. 1984. Functional and regulatory properties of H^+-pumps at the tonoplast and plasma membranes of *Zea mays* coleoptiles. *Z. Naturforsch.* **39c:**927–937
32. Hansen, U.-P., Warncke, J., Keunecke, P. 1973. Photoelectric effects in characean cells. *Biophysik* **9:**197–207
33. Hansen, U.-P., Gradmann, D., Sanders, D., Slaymann, C.L. 1981. Interpretation of current-voltage relationships for active ion transport systems I. *J. Membrane Biol.* **63:**165–190
34. Hansen, U.-P., Tittor, J., Gradmann, D. 1983. Interpretation of current-voltage relationship for active ion transport systems II. *J. Membrane Biol.* **75:**141–169
35. Hansen, U.-P. 1987. Relationship between photosynthesis and plasmalemma transport. *J. Exp. Bot.* **38:**1965–1981
36. Hansen, U.-P. 1990. Implications of control theory for homeostasis and phosphorylation of transport molecules. *Bot. Acta* **103:**15–23
37. Hansen, U.-P., Moldaenke, C., Tabrizi, H.A., Ramm, D. 1993. The effect of transthylakoid proton uptake on cytosolic pH and the imbalance of ATP and NAPDH/H^+ production as measured by CO_2- and light-induced depolarisation of the plasmalemma. *Plant Cell Physiol.* **34:**681–695
38. Hedrich, R., Moran, O., Conti, F., Busch, H., Becker, D., Gambale, F., Dreyer, I. Küch, A., Neuwinger, K. 1995. Inward rectifier potassium channels differ from their animal counterparts in response to voltage and channel modulators. *Eur. Biophys. J.* **23:**1–9
39. Hodgkin, A.L., Katz, B. 1949. The effect of sodium ions on the electrical activity of the giant axon of the squid. *J. Physiol.* **108:**37–77
40. Jeschke, W.D. 1967. Die cyclische und die nichtcylcische Photophosphorylierung als Energie-quelle der lichtabhängigen Chloridaufnahme bei *Elodea densa. Planta* **73:**161–174
41. Kuschel, L., Dahse, I., Müller, E. 1996. Lack of correlation between transplasmalemma electron transport rate and depolarisation in *Egeria densa* leaf cells. *J. Plant Physiol.* **147:**675–684
42. Lucas, W.J. 1983. Photosynthetic assimilation of exogenous HCO_3^- by aquatic plants. *Ann. Rev. Plant Physiol.* **34:**71–104
43. Lucas, W.J., Ogata, K. 1985. Hydroxyl- and bicarbonate-associated transport processes in *Chara corallina. J. Exp. Bot.* **36:**1947–1958
44. Madsen, T.V., Sand-Jensen, K. 1991. Photosynthetic carbon assimilation in aquatic macrophytes. *Aquatic Botany* **41:**5–40
45. Marrè, M.T., Albergoni, F.G., Moroni, A., Pugliarello, E. 1989. Evidence that H^+ extrusion in *Elodea densa* leaves is mediated by an ATP-driven H^+ pump. *Plant Sci.* **62:**21–28
46. Marrè, M.T., Albergoni, F.G., Moroni, A., Marré, E. 1989. Light-induced activation of electrogenic H^+ extrusion and K^+ uptake in *Elodea densa* depends on photosynthesis and is mediated by the plasma membrane H^+ ATPase. *J. Exp. Bot.* **40:**343–352
47. Marré, E., Rasi-Caldogno, F. 1989. Metabolism-transport interactions. *In:* Plant membrane transport J. Dainty, M.I.D. Michaelis, E. Marré, F. Rasi-Caldogno, editors. pp. 307–316. Elsevier, Amsterdam
48. Marré, E., Marré, M.T., Moroni, A., Venegoni, A., Vergani, P., Albergoni, F. 1994. Metabolism-mediated control of ATP-driven H^+ extrusion. *In:* Biochemical mechanisms involved in plant growth regulation. C.J. Smith, J. Gallon, D. Chiatante, G. Zocchi, editors. pp. 245–258. University Press, Oxford
49. Miedema, H., Felle, H., Prins., H.B.A. 1992. Effect of high pH on the plasma membrane potential and conductance in *Elodea densa. J. Membrane Biol.* **128:**63–69
50. Miedema, H., Prins, H.B.A. 1993. Simulation of the light-induced oscillations of the membrane potential in *Potamogeton* leaf cells. *J. Membrane Biol.* **133:**107–117
51. Mummert, H., Gradmann, D. 1991. Action potentials in *Acetabularia:* Measurement and simulation of voltage-gated fluxes. *J. Membrane Biol.* **124:**265–273
52. Natura, G., Schmidt, C., Traber, H., Sack, H., Dahse, I., Müller, E. 1995. Potassium channels of *Egeria* leaf cells are pH-sensitive. 10th International Workshop of Plant Membrane Biology, C40, 6–11.8.1995 Regensburg
53. Nedler, J.A., Mead, R. 1965. A Simplex method for function minimization. *Computer Journal* **7:**308–313
54. Okazaki, Y., Tazawa, M., Iwasaki, N. 1994. Light-induced changes in cytosolic pH in leaf cells of *Egeria densa. Plant Cell Physiol.* **35:**943–950
55. Petzold, U., Dahse, I., Müller, E. 1985. Light-stimulated electrogenic uptake of neutral amino acids by leaf cells of *Egeria densa* and *Vicia faba. Biochem. Physiol. Pflanzen* **180:**655–666
56. Plieth, C., Tabrizi, H., Hansen, U.-P. 1994. Relationship between banding and photosynthetic activity in *Chara corallina* as studied by the spatially different induction curves of chlorophyll fluorescence observed by an image analysis system. *Physiol. Plant.* **91:**205–211
57. Prins, H.B.A., Elzenga, J.T.M. 1989. Bicarbonate utilization: Function and mechanism. *Aquatic Botany* **34:**59–83
58. Rascio, N., Mariani, P., Tommasini, E., Bodner, M., Larcher, W. 1991. Photosynthetic strategies in leaves and stems of *Egeria densa. Planta* **185:**297–303
59. Sanders, D. 1980. The mechanism of Cl^- transport at the plasma membrane of *Chara corallina. J. Membrane Biol.* **53:**129–141
60. Sanders, D., Hansen, U.-P. 1981. Mechanism of Cl^- transport at the plasma membrane of *Chara corallina. J. Membrane Biol.* **58:**139–153
61. Sanders, D. 1984. Gradient-coupled chloride transport in plant cells. *In:* Chloride Transport Coupling in Biological Membranes and Epithelia. A. Gerencser, editor. pp. 63–120. Elsevier, Amsterdam
62. Sanders, D. 1990. Kinetic modeling of plant and fungal membrane transport systems. *Annu. Rev. Plant Physiol.* **41:**77–107
63. Schultz, S.G. 1980. Basic principles of membrane transport. University Press, Cambridge
64. Schwefel, H.P. 1977. Numerische Optimierung von Computer-Modellen mittels der Evolutionsstrategie. Birkhäuser-Verlag, Basel
65. Serrano, R. 1989. Structure and function of plasma membrane ATPase. *Annu. Rev. Plant Physiol. Plant Mol. Biol.* **40:**61–94
66. Spanswick, R.M. 1972. Electrical coupling between cells of higher plants. *Planta* **102:**215–227
67. Staal, M., Elzenga, J.T.M., Prins, H.B.A. 1989. ^{14}C Fixation by leaves and leaf cell protoplasts of the submerged aquatic angiosperm *Potamogeton lucens L.*: carbon dioxide or bicarbonate? *Plant Physiol.* **90:**1035–1040

68. Stewart, P.A. 1983. Modern quantitative acid-base chemistry. *Can. J. Physiol. Pharmacol.* **61:**1444–1461
69. Tazawa, M., Shimmen, T., Mimura, T. 1986. Action spectrum of light-induced membrane hyperpolarization in *Egeria densa*. *Plant Cell Physiol.* **27:**163–168
70. Thiel, G., Gradmann, D. 1994. Electrophysiology of stomata. *Progress in Botany* **55:**59–78
71. Tyerman, S.D., Findlay, G.P., Paterson, G.J. 1986. Inward membrane current in *Chara inflata*. *J. Membrane Biol.* **89:**153–161
72. Vanselow, K.H., Dau, H., Hansen, U.-P. 1988. Indication of transthylakoid proton-fluxes in *Aegopodium podagraria L.* by light-induced changes of plasmalemma potential, chlorophyll fluorescence and light-scattering. *Planta* **176:**351–361
73. Vanselow, K.H., Hansen, U.-P. 1989. Rapid effect of light on the K^+-channel in the plasmalemma of *Nitella*. *J. Membrane Biol.* **110:**175–187
74. Vanselow, K.H., Kolbowski, J., Hansen, U.-P. 1989. Further evidence for the relationship between light-induced changes of plasmalemma transport and transthylakoid proton uptake. *J. Exp. Bot.* **40:**239–245
75. Weigl, J. 1967. Beweis für die Beteiligung von beweglichen Transportstrukturen beim Ionentransport durch pflanzliche Membranen und die Kinetik des Anionentransportes bei *Elodea* im Licht und Dunkeln. *Planta* **75:**327–342
76. Weisenseel, M.H., Linder, B. 1990. Polar current patterns in the leaves of the aquatic angiosperm *Elodea canadensis*. *Protoplasma* **157:**193–202

Appendix 1

Summary of the Main Model Equations

1. Open Probabilities

$$P_P(t) = K \cdot \sum M_i \quad \text{with} \tag{19}$$

$$dM_i/dt = -1/\tau_i \cdot M_i(t) + K_i/\tau_i \cdot L_A, \quad i = \overline{1,3} \tag{20}$$

$$dP_i/dt = -k_i^i \cdot P_i + k_i^a \cdot (1 - P_i), \quad i \in \{Ki,Ko,Cl,SP,H\} \quad \text{with} \tag{21}$$

$$k_i^a = \hat{k}_i^a \cdot \exp(\delta_i^a \cdot FE_M/(RT)) \tag{22}$$

$$k_i^i = \hat{k}_i^i \cdot \exp(\delta_i^i \cdot FE_M/(RT)) \tag{23}$$

2. Membrane Potential

$$dE_M/dt = 1/C_M \cdot \sum i_i \tag{24}$$

3. Current Densities

$$i_i = g_i \cdot (E_M - E_i) \tag{25}$$

4. Conductances

$$g_i = g_i^{\max} \cdot P_i \quad \text{with} \tag{26}$$

$$g_i^{\max} = g_i^0 \cdot \gamma_i \tag{27}$$

5. Reversal Potentials

$$E_i = -\frac{RT}{z_i F} \ln \frac{c_i^{cyt}}{c_i^{ext}}, \quad i \in \{K,Cl,H\} \tag{28}$$

$$E_{SP} = 2E_H - E_{Cl} \tag{29}$$

$$E_P = E_{ATP} + E_H \quad \text{with} \quad E_{ATP} = \frac{-\Delta G_{ATP}}{s \cdot F}. \tag{30}$$

Appendix 2

Model Parameters

Table *A*1. General model parameter

Parameter	Symbol	Value	Reference
Cytosolic pH	pH^{cyt}	7.3	[2, 54]
Cytosolic K^+ concentration	c_K^{cyt}	200 mM	[17]
Cytosolic Cl^- concentration	c_{Cl}^{cyt}	46 mM	[17]
Free energy of ATP hydrolysis	ΔG_{ATP}	−50 kJ/mol	[7, 12]
Specific membrane capacitance	C_M	1 μF/cm^2	[34]

Table *A*2. Parameter of the model transporter

	K	K_1	K_2	K_3
Proton pump	0.01	0.03	−0.7	0.66
	δ_i^a	δ_i^i	$\hat{k}_i^a$ [s^{-1}]	$\hat{k}_i^i$ [s^{-1}]
H^+ channel	−0.5	0.5	0.0050	29.00
K^+-inward rectifier	−0.5	0.5	0.0012	22.00
K^+-outward rectifier	0.5	−0.5	0.1000	0.03
Cl^- channel	0.5	−0.5	1.0000	0.09
$(2H\text{-}Cl)^+$ symporter	−0.5	0.5	0.0180	10.00

Table *A*3. Basic maximum conductances g_i^o of K^+- and Cl^--transporters

	c_K^{ext} [mol/m^3]	c_{Cl}^{ext} [mol/m^3]	$g_{Ki}^o = g_{Ko}^o$ [S/m^2]	g_{Cl}^o [S/m^2]	g_{SP}^o [S/m^2]
A	1.0	1.0	1.0	0.100	0.020
B	0.1	3.6	0.5	0.120	0.024
B	1.0	4.5	1.0	0.125	0.025
B	10.0	13.5	3.0	0.150	0.030

A: Simulation of the light effect on membrane potential; B: Simulation of medium pH- and KCl-dependence of the membrane potential.

Table *A*4. Time constants τ_i and amplitude factors A_i achieved by curve-fitting of the response of the membrane potential to a stepwise change in light intensity on Eq. 1

	τ_i [s]	A_i [mV]	$\check{\tau}_i$ [s]
1	29.43 ± 6.61	18.07 ± 6.95	5..40
2	263.95 ± 21.74	−344.33 ± 48.10	180..600
3	307.19 ± 22.67	316.47 ± 50.46	

In the last column corresponding time constants $\check{\tau}_i$ from other plants [37] are shown.